

## Comparative study on path interval determinations in filleted end milling

Tsutomu Sekine\* and Kyoko Kameya

Department of Systems Design Engineering, Faculty of Science and Technology, Seikei University, Tokyo 180-8633, Japan

Received 9 June 2021  
Revised 17 August 2021  
Accepted 15 September 2021

### Abstract

This study provides several findings obtained from the comparisons of path interval determinations in filleted end milling with a tool inclination. CNC milling machine is one of the core technologies in practical manufacturing. Computer-aided technologies have contributed to the technological advancement. Tool path generation in computer-aided manufacturing is really important for CNC milling process. Although there are a lot of parameters treated in tool path generation, path interval is one of the influential factors in considering the balance between manufacturing efficiency and machined surface feature. A path interval determination in filleted end milling always includes the intersection problems with mathematical complexities in essence. To overcome the complexities, the related studies have been made so far. However, it is considerably difficult to search a study comparing the path interval determinations of filleted end milling, and this fact is making it difficult to select a suitable path interval determination in practice. Accordingly, this study focused on comparing four possible procedures of the path interval determinations. After the comparative discussions were made using the results using the four possible procedures, the several findings were revealed according to the explicit evidences.

**Keywords:** Tool path generation, Path interval, Multi-axis CNC machining, Filleted end mill, Modeling error

### 1. Introduction

Digital twin is one of the next-generation technologies having innovative potential to simulate, predict, and optimize manufacturing systems and processes. The high expectations are actually growing in industrial society [1]. Simulation technologies based on the real-time data have been gradually developed, and the practical applicability has also been enhanced to create various digital models with high accuracy [2, 3]. These days, the growing demands is increasing more and more to establish a new platform in various fields [4].

The smart manufacturing and Industry 4.0 including Digital Twin are well-known concepts and direct trigger in the development of manufacturing platform [5-7]. The recent advances of information and communication technologies are adding impetus to the concepts' dissemination in our society. Moreover, the relative concepts, such as "Industrial Internet of Things," have been made one after another. Even in the field of machine tools, Machine tool 4.0 was proposed as a derivative concept including internet of things and cloud computing applied to computer numerically controlled (CNC) machine tools [8], while the accuracy improvement of each relative element in machine tools has a valuable potential to enhance the performance of manufacturing technologies in both real and digital space.

CNC machine tools gain widespread use in today's industry [9-11]. Although simulation technologies supporting Digital Twin is expected to inspire further innovation in production system, its maximum benefit would be unobtainable without product manufacturing under the optimum condition. Milling is one of the manufacturing processes having notable compatibility with CNC machine tools. The compatibility is also supported strongly by computer-aided technologies Computer-aided design (CAD) has played a central role in shape design process [12], whereas computer-aided manufacturing (CAM) has also played an important role in product manufacturing with CNC machine tools [13, 14]. In the process planning, the machine movement is produced by CAM, and the quality leads to great influence on surface feature, machining efficiency, etc. Accordingly, further advanced milling has significantly focused on tool path generation to achieve higher machining speeds and longer tool life [15-17].

There are a lot of setting parameters in tool path generation. Among them, path interval is one of the influential factors in considering the balance between manufacturing efficiency and machined surface feature. The related studies have usually focused on two path intervals in milling [18]. Those are a path interval along both the feed direction of a tool and the cross-feed direction of a tool. Path interval determination have mainly dealt with the latter [19, 20]. To predict a proper path interval, scallop height is used as a control variable. Here, there are various kinds of milling tools in these days. Among them, several tools with typical tool tip geometries have been investigated in path interval determination. For instance, a half circle can be applicable for the tool tip geometry of ball end mill when the tool having contact at a point on a designed shape is projected onto an instantaneous section defined according to both tool path and tool posture [21, 22]. In the procedure, an intersection problem can be solved using a designed shape and two half circles based on adjacent tool paths. Useful formulas were proposed through the geometrical consideration, and a suitable path interval or scallop height could be obtained in ball end milling [23, 24].

\*Corresponding author. Tel.: +814 2237 3710  
Email address: ts\_s@outlook.com  
doi: 10.14456/easr.2022.38

Multi-axis flat and filleted end milling become necessary to create different insight. Advanced treatment is required in the geometrical modelling of cutting edge geometries. These profiles projected onto an instantaneous section change circumstantially with a variation of both tool path and tool posture [25, 26]. The procedures with wide applicability, robustness, efficiency, and accuracy was reported to determine a proper path interval in multi-axis flat end milling [27].

On the other hand, the machining situations in multi-axis filleted end milling can be classified into four general groups [28]. Although the related study has been reported to provide a suitable path interval in filleted end milling with tool inclination along a tool feed direction [29, 30], grabbing the geometrical insight was extremely difficult in the two-dimensional expression. The three-dimensional (3D) expression can provide a deliberate solution even if there are mathematical complexities entailed in intersection problems of 3D geometries [31]. A novel procedure focusing on a reference point was proposed to enhance predictiveness of path interval determination in filleted end milling with a tool inclination [32]. The findings indicated that introducing the reference point was beneficial to calculate a path interval correctly. However, the study dealt with several tool geometries to estimate a path interval. Hence, the more detailed investigation is essential to reveal the further characteristics for practical application.

The purpose of this study is to investigate and compare the accuracies of several approaches for path interval determination in filleted end milling with tool inclination. The experiments were also conducted to reveal a path interval determination with high accuracy. The discussion is made based on the comparative results. After that, some conclusions are drawn to achieve a suitable path interval in multi-axis filleted end milling.

---

Algorithm: Path interval determination

Input:  $R, R_{cr}, \rho, h$

Output:  $L / 2$

- 1: Set  $\mathbf{X}, \mathbf{Y}, \mathbf{Z}, \mathbf{XT}, \mathbf{YT}, \mathbf{ZT}, \mathbf{n}_h, \mathbf{P}_{base}$ , and  $\mathbf{t}_{base}$
  - 2: Calculate  $\gamma_{ap}$  using Eq. (1)
  - 3: Calculate  $\eta$  using Eq. (2)
  - 4: Calculate  $d_s$  using Eq. (3)
  - 5: Set a search range  $\mathbf{P}_{start}$  and  $\mathbf{P}_{end}$   
for the following iterative calculation
  - 6: do
  - 7: Update  $\gamma$  according to  $R_{cr} - d_s$
  - 8: Update  $\mathbf{P}_{ap}$  and  $\mathbf{t}_{ap}$
  - 9: Calculate  $\eta$  using Eq. (2)
  - 10: Calculate  $d_s$  using Eq. (3)
  - 11: while  $|R_{cr} - d_s| \geq \varepsilon$
  - 12:  $\mathbf{m}_{sep} \leftarrow \mathbf{t}_{sep} \times \mathbf{n}_h, \mathbf{u}_{sep} \leftarrow \mathbf{t}_{sep} \times \mathbf{m}_{sep}$
  - 13:  $\mathbf{P}_{hp} \leftarrow \mathbf{P}_{sep} + R_{cr} \mathbf{u}_{sep}$
  - 14:  $\gamma_{scp} \leftarrow \gamma$
  - 15: Calculate  $\gamma$  using Y-axis component of  $\mathbf{P}_{sep}$   
to set a search range for the next iterative calculation
  - 16: Let  $\mathbf{P}_{hp} [1 \dots n]$  and  $\gamma [1 \dots n]$  be new arrays  
through dividing the search range from  $\gamma$  to  $\gamma_{scp}$   
into appropriate even numbers
  - 17:  $\gamma [1] \leftarrow \gamma, \gamma [n] \leftarrow \gamma_{scp}$
  - 18: Calculate  $\mathbf{P}_{hp} [1]$  and  $\mathbf{P}_{hp} [n]$
  - 19: do
  - 20: for  $i = 2$  to  $n - 1$
  - 21: Calculate  $\gamma [i]$  and  $\mathbf{P}_{hp} [i]$
  - 22: end for
  - 23: Find  $\mathbf{P}_{hp} [i]$  with the maximum of Y-axis component
  - 23: Rearrange  $\mathbf{P}_{hp} [1]$  and  $\mathbf{P}_{hp} [n]$  using the elements  
near  $\mathbf{P}_{hp} [i]$  calculated above, and update  $\gamma [1]$  and  $\gamma [n]$
  - 24: Compute the difference between  $\mathbf{P}_{hp} [i]$  calculated above  
and the adjacent  $\mathbf{P}_{hp} [i]$  in Y-axis component
  - 25: while the difference  $\geq \varepsilon$
  - 26:  $L / 2 \leftarrow \max \{ \text{Y-axis component of } \mathbf{P}_{hp} [i]: i = 1 \text{ to } n \}$
- 

**Figure 1** Computational algorithm [33]

**2. Path interval determinations in filleted end milling**

*2.1 A procedure using 3D geometrical computation*

In this section, an up-to-date procedure is provided to obtain a suitable path interval in filleted end milling. Figure 1 shows the pseudo-code of path interval determination [33]. The algorithm can be briefly explained as follows. Given that a cutting tool is inclined along a tool feed direction and the milling is performed on a plane to create a designed surface as shown in Figure 2, a path interval is commonly expressed as a distance between adjacent tool paths. Hereafter,  $L/2$  is used as a path interval, which is a unilateral distance from a tool center point to a section with predetermined scallop height  $h$ . An instantaneous state of filleted end milling can be described using a torus expressing geometrical features in the cutting edge geometry. This modeling specifies several radii i.e.  $R$ ,  $R_b$ , and  $R_{cr}$ , and an arbitrary inclination angle  $\rho$ . As shown in Figure 3, each axis of global coordinate system is given as  $\mathbf{X}$ ,  $\mathbf{Y}$ , and  $\mathbf{Z}$  whose components are set as  $(1, 0, 0)$ ,  $(0, 1, 0)$ , and  $(0, 0, 1)$ , respectively.  $\mathbf{XT}$ ,  $\mathbf{YT}$ , and  $\mathbf{ZT}$  are also set the axes of tool coordinate system. The direction of  $\mathbf{YT}$  axis is the same as that of  $\mathbf{Y}$  axis, and tool feed direction coincides with the direction of  $\mathbf{X}$  axis. Two planes are introduced as a designed surface and  $h$  pseudo plane. The distance of two planes becomes  $h$  in any position. Moreover,  $\mathbf{n}_h$  is a surface normal of  $h$  pseudo plane. When the torus with inclination  $\rho$  has contact with a designed surface, a section can be created as an exact circle cut out from the torus. Three positional relationships can arise between a torus section and  $h$  pseudo plane. The one is an intersection between a torus section and  $h$  pseudo plane, while there exists a positional relationship without an intersection. The other situation is a single contact point between a torus section and  $h$  pseudo plane.

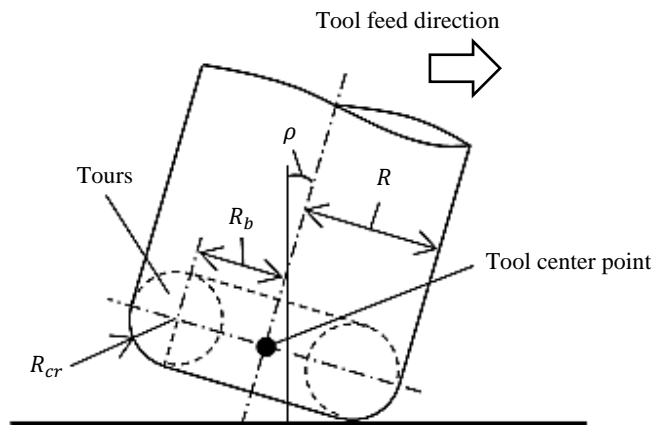


**Figure 2** Filleted end milling with a tool inclination angle  $\rho$  [33]

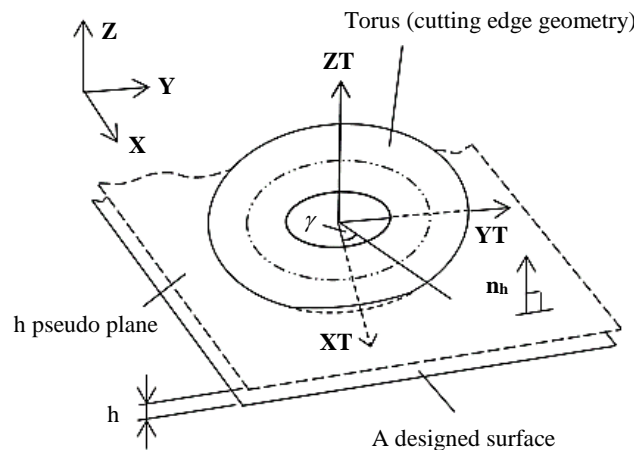


**Figure 3** Geometrical relationships between two planes and cutting edge geometry (torus) [33]

The notation  $\mathbf{P}$ ,  $\mathbf{t}$ , and  $\mathbf{u}$  mean a positional vector in 3D space, a tangent vector at each torus section's center, and a directional vector, respectively. The subscript base is assigned to some variables on a section including a contact point between the torus and a designed shape. The distance between  $\mathbf{P}_{base}$  and a designed shape is completely equal to  $R_{cr}$ . The subscript ap indicates an arbitrary position.  $\gamma$  is an angular parameter to determine an arbitrary position on a circle with  $R_b$ . The initial value of  $\gamma$ , i.e.  $\gamma_{ap}$  can be calculated using the following formula:

$$R_b \sin \rho - R_b \cos \gamma \sin \rho = 0.5h \tag{1}$$

An arbitrary position on the circle  $\mathbf{P}_{ap}$  can be calculated by iterative calculation along a circle with  $R_b$ .  $\epsilon$  is set as the convergence condition of iterative calculation. A tangent vector  $\mathbf{t}_{ap}$  can be also calculated using  $\mathbf{t}_{base}$  in the same manner. A direction cosine  $\eta$  between  $\mathbf{t}_{ap}$  and  $h$  pseudo plane can be obtained from the following equation:

$$\eta = \mathbf{t}_{ap} \cdot \{(\mathbf{n}_h \times \mathbf{t}_{ap}) \times \mathbf{n}_h\} \quad (2)$$

The following formula enables us to calculate a distance  $d_s$  between  $\mathbf{P}_{ap}$  and  $\mathbf{P}_{hp}$ :

$$d_s = \frac{(R_{cr} - h + R_b \sin \rho - R_b \cos \gamma \sin \rho)}{\eta} \quad (3)$$

The subscript scp in Figure 1 means a single contact point between a torus section and h pseudo plane.  $\mathbf{P}_{scp}$  and  $\mathbf{t}_{scp}$  are obtained through updating  $\mathbf{P}_{ap}$  and  $\mathbf{t}_{ap}$  in iterative calculation, which is the first do-while statement with the convergence condition  $\varepsilon$  in Figure 1.  $\mathbf{P}_{hp}$  represents a positional vector on h pseudo plane. To find a suitable path interval  $L/2$ , the other iterative calculation is performed according to the second iterative calculation in algorithm. The calculation can ascertain a single contact point between a torus section and h pseudo plane. Through finding out the farthest intersection from the tool center point, the algorithm can provide a suitable path interval  $L/2$ .

### 2.2 A procedure proposed by Sekine et al.

A path interval determination based on a projection of tool into an instantaneous section was proposed by Sekine et al [28]. The procedure defines an effective radius  $R_{eff}$  on an instantaneous section, as follows.

$$R_{eff} = \frac{R_{long}^2 + R_{short}^2}{2R_{short}} \quad (4)$$

where  $R_{long}$  and  $R_{short}$  are a long and short radius of ellipse to derive  $R_{eff}$ , and they can be calculated from the following equations:

$$R_{long} = \frac{R_{short}}{|\sin \rho|} \quad (5)$$

$$R_{short} = Z_{tc} - R_{cr} \cos \rho \quad (6)$$

In equation 6,  $Z_{tc}$  is a height at the center of tool. It can be obtained geometrically:

$$Z_{tc} = |R_b \sin \rho| + R_{cr} \quad (7)$$

From the above equations, a path interval  $L/2$  can be given in a similar manner to that in ball end milling [17]:

$$\frac{L}{2} = \sqrt{2R_{eff}h - h^2} \quad (8)$$

### 2.3 A procedure proposed by Redonnet et al.

Redonnet et al. also used a projection of tool into an instantaneous section, and the following effective radius was proposed to determine a path interval [34, 35]:

$$R_{eff} = \frac{R_b}{\sin \rho} + R_{cr} \quad (9)$$

In this procedure, a path interval  $L/2$  can be calculated using the equation 8 since the theoretical approach is one of the applications from that in ball end milling.

### 2.4 A procedure proposed by Bedi et al.

The alternative procedure using a projection of tool into an instantaneous section was proposed by Bedi et al [36]. In the procedure,  $R_{long}$  is provided as follows:

$$R_{long} = R_b + R_{cr} \sin \rho \quad (10)$$

After that, a path interval  $L/2$  is obtained in a similar manner to that in flat end milling [27]:

$$\frac{L}{2} = R_{long} \sqrt{1 - \left( \frac{R_{long} \sin \rho - h}{R_{long} \sin \rho} \right)^2} \quad (11)$$

Note that this section only deals with the partial procedures applicable for filleted end milling with a tool inclination along a tool feed direction, while the several procedures explained above can be available in the other conditions. In addition, we are assuming for simplicity that the milling process is performed on a plane.

### 3. Comparisons and discussion

This section describes the comparative results of several procedures to determine a path interval in filleted end milling with a tool inclination along a tool feed direction. Path intervals calculated from the procedures will be provided with numerical evidence. Then, the results of experimental verification will be added to identify a suitable path interval determination. After that, several discussions illuminate some measures to select a proper procedure for an effective filleted end milling. Hereafter, degrees are used as units to express tool inclination angle  $\rho$ .

Before several comparisons, proof-of-theory experiments were conducted with CNC milling machine whose type was PSF550-CNC with the mechanism of tilting spindle. Figure 4 shows the milling machine. The spindle of milling machine can be tilted with the available range from -30 to 90 deg. Tool inclination angle  $\rho$  was properly adjusted in accordance with each experimental condition. Filleted end mills (2RBE) made by FUKUDA SEIKO Co, Ltd. were individually attached to the spindle, and each radius of tools was  $R = 3.0$  and  $6.0$  mm. In addition, each radius of tool's cutting edges was  $R_{cr} = 1.0$  and  $2.0$  mm. A synthetic wood, SANMODUR MH-E, was used as a material to be machined. The material was attached to a vice on the machine's table. Table 1 shows the experimental conditions. The conditions were cautiously determined based on the results of preliminary experiments. In each experiment, a path interval  $L/2$  was numerically calculated under the two conditions of scallop height, i.e.,  $h = 0.05$  and  $0.10$  mm. The scanning line machining was executed only from one direction in each experiment. The milling processes in each experimental condition were performed three times to investigate the repeatability of machined surface feature.

After the experiments, a specimen was cut out from a machined material. Optical microscope (Mitutoyo TM-505) was used for the measurements after experiments. The cut-out specimen was set on the stage of microscope. Then, the scallop height was measured in each machined part. The average value was calculated after three measurements in each experimental condition. These values were compared with the calculated ones derived from the procedures explained above. In terms of practically-beneficial path interval determination in multi-axis filleted end milling, the accuracy and predictiveness will be discussed based on the results.

Table 2 shows path intervals  $L/2$  calculated from each procedure when  $R = 3$  mm and  $R_{cr} = 1$  mm. At first glance, the values of computational procedure were close to those of procedure by Bedi et al. In contrast, the other results were achieved as unique values depending on each approach. Table 3 shows path intervals  $L/2$  calculated from each procedure when  $R = 6$  mm and  $R_{cr} = 2$  mm. Although an isotropic, uniform increases arose in filleted end mill, it was found that there were the similar tendencies between each value in two tables.

In experimental verification, excellent agreement was achieved when a milling process was conducted according to a path interval derived through the computational procedure. Figure 5 is graphic comparisons of the experimental and computed values when  $R = 3$  mm and  $R_{cr} = 1$  mm, whereas Figure 6 is graphic comparisons of the both values when  $R = 6$  mm and  $R_{cr} = 2$  mm. In both figures, green bar graphs represent the experimental results, and white bar graphs indicate the predetermined values acting as each measure in the proof-of-theory experiments. It was obvious from Figure 5 that the procedure using 3D geometrical computation could estimate a suitable path interval with high accuracy even when tool inclination angle  $\rho$  changes according to a machining situation. In addition, each maximum deviation of experimental results indicated by green bar graph in Figure 5 was 0.002, 0.000, 0.004, and 0.001, respectively, from the left-sided one. The results demonstrated that the deviations were extremely small. It should be kept in mind that the experimental results provided to comparisons include several errors occurred with the experiments. Even though there exist the other unaware factors possible to reduce cutting accuracy, those values would not have a serious negative effect on machined surface features from practical perspective. Each maximum deviation of experimental results indicated by green bar graph in Figure 6 was 0.001, 0.003, 0.001, and 0.000, respectively, from the left-sided one. Hence, the similar interpretation were understandably made from the results in Figure 6. From the results in two figures and tables, it was undoubted that the procedure using 3D geometrical computation could properly offer an accurate path interval in filleted end milling with a tool inclination even if tool radius  $R$ , scallop height  $h$ , and tool inclination angle  $\rho$  were changed in practice.

On the basis of the experimental verification, the renewed attention was drawn to the comparisons between path intervals. In Tables 2 and 3, there are obvious differences between the results of computational procedure and those of procedure. The two tables also indicated that the results of procedure by Redonnet et al. included a certain amount of difference, respectively. In contrast, it was definite that the procedure by Bedi et al. could provide a path interval with practically-adequate accuracy, whereas it employed a projected ellipse on an instantaneous section created according to a machining state.

These numerical differences essentially come from the theory-creating process of geometrical modeling. There are two approaches in considering the geometrical modeling to solve an intersection problem regarding path interval determination in filleted end milling with a tool inclination. The one is 3D geometrical modeling, and the other is two-dimensional (2D) one. The computational procedure is one of 3D versatile approaches. In this case, the intersection problem is relatively complex compared with that in 2D one, so that computational treatment is a powerful tool applicable for various machining states with a variation of tool posture. Contrarily, the other procedures in this study take 2D approach considering a projection of tool as a profile on an instantaneous section. This approach can be additionally classified into two manners regarding tool's projection. True-circular approximation was applied in the procedures by both Sekine et al. and Redonnet et al. This manner can be extended to a machining state with a variation of tool posture [28, 34]. From the comparisons, it was revealed that using an effective radius was susceptible to the error in geometrical modeling. Elliptic projection was employed in the procedure by Bedi et al. Although a tool's projection into a 2D section was conducted in this manner, the comparative results represented that the manner could provide a path interval with numerically small error of geometrical modeling. However, note that the latter manner can only cover filleted end milling with a tool inclination along a tool feed direction [36].

The effects of the procedures on scallop height  $h$  were investigated as the next step. In the investigation, the value of path interval is constantly set as that obtained from computational procedure. Moreover, each value of  $h$  was derived through the following formulas: in true-circular approximation,

$$h = R_{\text{eff}} - \sqrt{R_{\text{eff}}^2 - \frac{L^2}{4}} \quad (12)$$

in elliptic projection,

$$h = R_{long} \sin \rho \left( 1 - \sqrt{1 - \left( \frac{L}{2R_{long}} \right)^2} \right) \quad (13)$$

Table 4 shows scallop heights  $h$  calculated from each procedure when  $R = 3$  mm and  $R_{cr} = 1$  mm. Table 5, furthermore, represents scallop heights  $h$  obtained from each procedure when  $R = 6$  mm and  $R_{cr} = 2$  mm. The comparative results denoted the same overall tendency as ones in path interval. In true-circular approximation, the errors of geometrical modeling tended to become relatively large values when  $\rho = 5$  deg. In elliptic projection, the similar features were identified under the condition with the small tool inclination angle, while the errors of geometrical modeling were quite small in the all conditions. Hence, the errors would not have a serious negative effect on machined surface features in practice. From a comprehensive perspective based on the all results above, the numerical difference of path intervals between the computational procedure and the elliptic projection can be practically negligible in scallop height's calculation when the value is less than 0.01 mm.



**Figure 4** A general view of CNC milling machine used in each experiment

**Table 1** Experimental conditions in each filleted end mill

Parameters	Tool 1	Tool 2
Tool radius $R$ [mm]	3.0	6.0
Tool tip radius $R_{cr}$ [mm]	1.0	2.0
Depth of cut [mm]	4.5	6.5
Tool rotational speed $S$ [ $\text{min}^{-1}$ ]	1400	1200
Feed rate $F$ [mm/min]	100	100

**Table 2** The comparison of path intervals  $L/2$  calculated from each procedure with variations of  $\rho$  and  $h$  when  $R = 3$  mm and  $R_{cr} = 1$  mm

Parameters	Condition 1	Condition 2	Condition 3	Condition 4
$\rho$ [deg.]	5		10	
$h$ [mm]	0.05	0.10	0.05	0.10
$L/2$ [mm] using 3D geometrical computation	1.442	1.879	1.083	1.479
$L/2$ [mm] using the procedure by Sekine et al.	1.086	1.534	0.785	1.108
$L/2$ [mm] using the procedure by Redonnet et al.	1.547	2.186	1.118	1.579
$L/2$ [mm] using the procedure by Bedi et al.	1.437	1.864	1.081	1.474

**Table 3** The comparison of path intervals  $L/2$  calculated from each procedure with variations of  $\rho$  and  $h$  when  $R = 6$  mm and  $R_{cr} = 2$  mm

Parameters	Condition 1	Condition 2	Condition 3	Condition 4
$\rho$ [deg.]	5		10	
$h$ [mm]	0.05	0.10	0.05	0.10
$L/2$ [mm] using 3D geometrical computation	2.115	2.883	1.558	2.167
$L/2$ [mm] using the procedure by Sekine et al.	1.536	2.171	1.112	1.571
$L/2$ [mm] using the procedure by Redonnet et al.	2.188	3.093	1.581	2.235
$L/2$ [mm] using the procedure by Bedi et al.	2.112	2.874	1.556	2.162

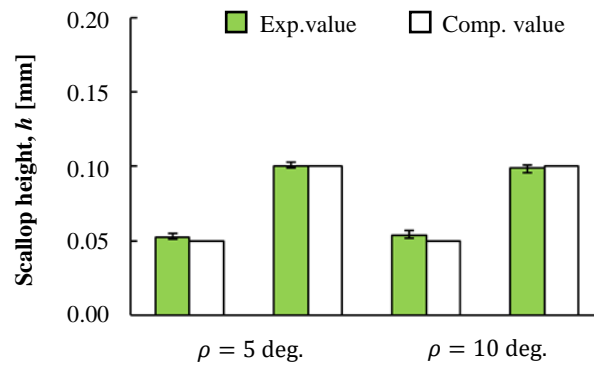


**Figure 5** The results of proof-of-theory experiments under the condition that  $R = 3$  mm and  $R_{cr} = 1$  mm [33]

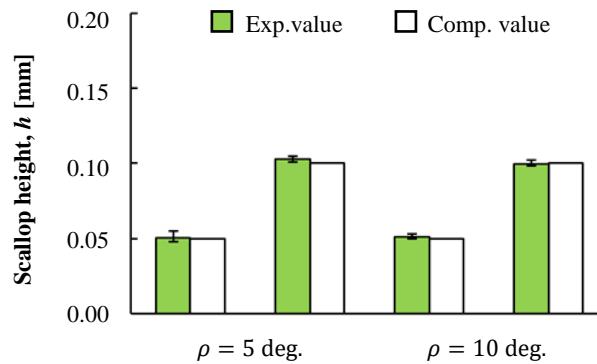


**Figure 6** The results of proof-of-theory experiments under the condition that  $R = 6$  mm and  $R_{cr} = 2$  mm [33]

**Table 4** The comparison of scallop height  $h$  calculated from each procedure with variations of  $\rho$  and  $L / 2$  based on 3D geometrical computation when  $R = 3$  mm and  $R_{cr} = 1$  mm

Parameters	Condition 1	Condition 2	Condition 3	Condition 4
$\rho$ [deg.]	5		10	
$L / 2$ [mm]	1.442	1.879	1.083	1.479
$h$ [mm] using 3D geometrical computation	0.050	0.100	0.050	0.100
$h$ [mm] using the procedure by Sekine et al.	0.088	0.150	0.096	0.179
$h$ [mm] using the procedure by Redonnet et al.	0.043	0.074	0.047	0.088
$h$ [mm] using the procedure by Bedi et al.	0.050	0.103	0.050	0.101

**Table 5** The comparison of scallop height  $h$  calculated from each procedure with variations of  $\rho$  and  $L / 2$  based on 3D geometrical computation when  $R = 6$  mm and  $R_{cr} = 2$  mm

Parameters	Condition 1	Condition 2	Condition 3	Condition 4
$\rho$ [deg.]	5		10	
$L / 2$ [mm]	2.115	2.883	1.558	2.167
$h$ [mm] using 3D geometrical computation	0.050	0.100	0.050	0.100
$h$ [mm] using the procedure by Sekine et al.	0.095	0.177	0.098	0.191
$h$ [mm] using the procedure by Redonnet et al.	0.047	0.087	0.049	0.094
$h$ [mm] using the procedure by Bedi et al.	0.050	0.101	0.050	0.100

**4. Conclusions**

This study compared path interval determinations in filleted end milling with a tool inclination along a tool feed direction. Four possible approaches for the path interval determination were focused on, and the procedures were explained with reference to the related studies. After comparative discussions were made from the results based on the procedures, the several findings were revealed according to the explicit evidences. Consequently, the following conclusions were drawn to achieve a suitable path interval determination in multi-axis filleted end milling.

- (1) The computational procedure can provide a suitable path interval determination with high accuracy in filleted end milling. Each maximum deviation of experimental results was adequately small values, and it was experimentally definite to achieve the desired accuracy in the path interval determination.
- (2) The true-circular approximation is susceptible to the error caused by 2D geometrical modeling, whereas the elliptic projection can offer a path interval with the numerically small error under milling process with a tool inclination along a tool feed direction.
- (3) The numerical difference of path intervals between the computational procedure and the elliptic projection can be practically negligible in scallop height's calculation when the value is less than 0.01 mm.

## 5. Acknowledgements

The authors would like to thank the financial support provided by OSG Fund, Shotoku Science Foundation, and the research grant from Faculty of Science and Technology, Seikei University.

## 6. References

- [1] Liu M, Fang S, Dong H, Xu C. Review of digital twin about concepts, technologies, and industrial applications. *J Manuf Syst.* 2020;58:346-61.
- [2] Phanden RK, Sharma P, Dubey A. A review on simulation in digital twin for aerospace, manufacturing and robotics. *Mater Today Proc.* 2021;38(9):174-8.
- [3] Cimino C, Negri E, Fumagalli L. Review of digital twin applications in manufacturing. *Comput Ind.* 2019;113:103130.
- [4] Jones D, Snider C, Nassehi A, Yon J, Hicks B. Characterising the digital twin: a systematic literature review. *CIRP J Manuf Sci Tech.* 2020;29:36-52.
- [5] Lu Y, Liu C, Wang KI, Huang H, Xu X. Digital twin-driven smart manufacturing: connotation, reference model, applications and research issues. *Robot Comput Integr Manuf.* 2020;61:101837.
- [6] Oztemel E, Gursev S. Literature review of Industry 4.0 and related technologies. *J Intell Manuf.* 2020;31:127-82.
- [7] Alcacer V, Cruz-Machado V. Scanning the Industry 4.0: a literature review on technologies for manufacturing systems. *Eng Sci Tech Int J.* 2019;22(3):899-919.
- [8] Liu C, Xu X. Cyber-physical machine tool-the era of machine tool 4.0. *Procedia CIRP.* 2017;63:70-5.
- [9] Jędrzejewski J. Machine tool development from high level of holistic improvement to intelligence. *J Achiev Mater Manuf Eng.* 2015;73:55-64.
- [10] Neugebauer R, Denkena B, Wegener K. Mechatronic systems for machine tools. *CIRP Ann Manuf Tech.* 2007;56(2):657-86.
- [11] Fujishima M, Mori M, Nishimura K, Ohno K. Study on quality improvement of machine tools. *Procedia CIRP.* 2017;59:156-9.
- [12] Alghazzawi TF. Advancements in CAD/CAM technology: options for practical implementation. *J Prosthodont Res.* 2016;60(2):72-84.
- [13] Lasemi A, Xue D, Gu P. Recent development in CNC machining of freeform surfaces: a state-of-the-art review. *Comput Aided Des.* 2010;42(7):641-54.
- [14] Konobrytskyi D, Hossain MM, Tucker TM, Tarbutton JA, Kurfess TR. 5-Axis tool path planning based on highly parallel discrete volumetric geometry representation: part I contact point generation. *Comput Aided Des Appl.* 2018;15(1):76-89.
- [15] Bo P, Barton M, Plakhotnik D, Pottmann H. Towards efficient 5-axis flank CNC machining of free-form surfaces via fitting envelopes of surfaces of revolution. *Comput Aided Des.* 2016;79:1-11.
- [16] Harik RF, Gong H, Bernard A. 5-axis flank milling: a state-of-the-art review. *Comput Aided Des.* 2013;45(3):796-808.
- [17] Sekine T, Obikawa T. Normal-unit-vector-based tool path generation using a modified local interpolation for ball-end milling. *J Adv Mech Des Syst Manuf.* 2010;4(7):1246-60.
- [18] Layegh E, Lazoglu I. 3D surface topography analysis in 5-axis ball-end milling. *CIRP Ann.* 2017;66:133-6.
- [19] Choi YK, Banerjee A, Lee JW. Tool path generation for free form surfaces using Bezier curves/surfaces. *Comput Ind Eng.* 2007;52(4):486-501.
- [20] Obikawa T, Sekine T. A higher-order formula of path interval for tool-path generation. *Int J Autom Tech.* 2011;5:663-8.
- [21] Tunc LT. Smart tool path generation for 5-axis ball-end milling of sculptured surfaces using process models. *Robot Comput Integr Manuf.* 2019;56:212-21.
- [22] Huang Y, Oliver JH. Non-constant parameter NC tool path generation on sculptured surfaces. *Int J Adv Manuf Tech.* 1994;9:281-90.
- [23] Mladenovic GM, Tanovic LM, Ehmann KF. Tool path generation for milling of free form surfaces with feedrate scheduling. *FME Trans.* 2015;43(1):9-15.
- [24] Chen T, Shi Z. A tool path generation strategy for three-axis ball-end milling of free-form surfaces. *J Mater Process Tech.* 2008;208(1):259-63.
- [25] Sarma R. Flat-Ended tool swept sections for five-axis NC machining of sculptured surfaces. *J Manuf Sci Eng.* 2000;122(1):158-65.
- [26] Plakhotnik D, Lauwers B. Computing of the actual shape of removed material for five-axis flat-end milling. *Comput Aided Des.* 2012;44(11):1103-14.
- [27] Sekine T, Obikawa T. Novel path interval determination in 5-axis flat end milling. *Appl Math Model.* 2015;39(12):3459-80.
- [28] Sekine T, Obikawa T, Hoshino M. Establishing a novel model for 5-axis milling with filleted end mill. *J Adv Mech Des Syst Manuf.* 2012;6:296-309.
- [29] Lin Z, Fu J, Shen H, Gan W. A generic uniform scallop tool path generation method for five-axis machining of freeform surface. *Comput Aided Des.* 2014;56:120-32.
- [30] Tourmier C, Duc E. Iso-scallop tool path generation in 5-axis milling. *Int J Adv Manuf Tech.* 2005;25(9):867-75.
- [31] Sekine T. A 3D geometrical consideration of path interval in filleted end milling. *J Jpn Soc Abras Tech.* 2016;60:515-9.
- [32] Sekine T. A computational algorithm for path interval determination in multi-axis filleted end milling. *Adv Sci Tech Res J.* 2020;14:198-205.
- [33] Sekine T, Kameya K. Remarkable characteristics of a novel path interval determination in filleted end milling. *Journal Européen des Systèmes Automatisés.* 2021;54(3):461-8.
- [34] Redonnet JM, Djebali S, Segonds S, Senatore J, Rubio W. Study of the effective cutter radius for end milling of free-form surfaces using a torus milling cutter. *Comput Aided Des.* 2013;45(6):951-62.
- [35] Segonds S, Seitier P, Bordreuil C, Bugarin F, Rubio W, Redonnet JM. An analytical model taking feed rate effect into consideration for scallop height calculation in milling with torus-end cutter. *J Intell Manuf.* 2019;30(5):1881-93.
- [36] Bedi S, Ismail F, Mahjoob MJ, Chen Y. Toroidal versus ball nose and flat bottom end mills. *Int J Adv Manuf Tech.* 1997;13:326-32.